COORDINATING VEHICLE PLATOONS FOR HIGHWAY BOTTLENECK DECONGESTION AND THROUGHPUT IMPROVEMENT

Mladen Čičić
Division of Decision and Control Systems
School of Electrical Engineering and Computer Science
KTH Royal Institute of Technology
Malvinas väg 10, 10044 Stockholm, Sweden
cicic@kth.se

Li Jin
Department of Civil and Urban Engineering
C2SMART University Transportation Center
New York University Tandon School of Engineering
15 MetroTech Center, Brooklyn, NY 11201, USA
lijin@nyu.edu

Karl Henrik Johansson
Division of Decision and Control Systems
School of Electrical Engineering and Computer Science
KTH Royal Institute of Technology
Malvinas väg 10, 10044 Stockholm, Sweden
kallej@kth.se

ABSTRACT

Truck platooning is a technology that is expected to become widespread in the coming years. Apart from the numerous benefits that it brings, its potential effects on the overall traffic situation needs to be studied further, especially at bottlenecks and ramps. However, assuming we can control the truck platoons from the infrastructure, they can be used as controlled moving bottlenecks, actuating control actions on the rest of the traffic. Thus properly controlled platoons can possibly improve the efficiency and throughput of the whole system. In this paper, we use a multi-class cell transmission model to capture the interaction between truck platoons and background traffic, and propose a corresponding queuing model, which we use for control design. As control inputs, we use platoon speeds, and the number of lanes platoons occupy, and we devise a control strategy for throughput improvement. This control law is applied on a highway section upstream of a bottleneck, with one on- ramp and one off-ramp. By postponing and shaping the inflow to the bottleneck, we are able to keep it in free flow, avoiding traffic breakdown and capacity drop, leading to significant reduction of total time spent of all vehicles. We tested the proposed control in a simulation study and found that by applying, we reduce the median delay of all vehicles by 75.6%. Notably, although they are slowed down while actuating control actions, platoons experience less delay compared to the case without control, since they avoid going through congestion at the bottleneck.

Keywords: Platooning, bottleneck, traffic control, multi-class, queuing

1 INTRODUCTION

With truck platooning progressing persistently towards becoming a commonplace technology [1], studying and understanding the impact it will have on the overall traffic is becoming increasingly important. Apart from providing potential fuel savings through air drag reduction [2], which was traditionally seen as its primary purpose, truck platooning is also expected have a positive impact on traffic efficiency through reducing the headways between vehicles [3, 4], alleviating the adverse effect trucks have on the traffic [5]. Although there have been numerous field tests of truck platooning in real traffic [6, 7], insufficient emphasis has been put on understanding how these platoons affect the behavior of other vehicles on the road; thus the possible drawbacks of this technology are not yet fully understood [8].

One identified problem pertains to the interaction between truck platoons and passenger cars close to on- and off-ramps, and bottlenecks in general [9]. There is concern that long platoons might block access to an off-ramp, or from an on-ramp, forcing drivers to slow down excessively or cut into a platoon, resulting in significant disturbances for both the platoon and the rest of the traffic. Furthermore, the arrival of platoons can cause traffic breakdown at a bottleneck, causing reduction of throughput due to the capacity drop phenomenon. Recently, there have been efforts to address this problem in microscopic [10, 11] and macroscopic [12] frameworks. In this paper, we are focusing on applying a new type of macroscopic control, using the truck platoons as actuators.

Bottleneck decongestion has long been tackled by classical traffic control measures, such as ramp metering [13] and variable speed limits [14]. However, both of these control methods require additional fixed equipment to be installed upstream of the bottleneck, which limits their flexibility, especially when it comes to handling temporary bottlenecks, such as work zones, incidents etc. With the introduction of connected autonomous vehicles to the highways, new opportunities for sensing [15] and actuation [16, 17] of the traffic are becoming available. Lagrangian actuation, where we use a subset of vehicles that can be controlled directly from the infrastructure to restrict the traffic flow, is lately garnering some attention [18–20]. This approach effectively emulates ramp metering and variable speed control, achieving a similar type of regulation without the need for additional fixed equipment, allowing us to also control areas away from known permanent bottlenecks. Moving bottleneck control is one such method, where we use slower moving vehicles to restrict the mainstream traffic flow at some points, delaying the arrival of some vehicles in a way similar to ramp metering and variable speed limits.

Due to their large size and the existence of fleet management infrastructure, truck platoons are an ideal candidate for moving bottleneck control. Since they consist of heavy, slow-moving vehicles, truck platoons will act as moving bottlenecks with or without external control, and we may use the communication channels already in place to send centrally computed reference speeds and other control actions [21]. This way, we are able to mitigate the negative effects trucks have on the traffic, and even improve the overall traffic situation. Apart from these positive effects on the traffic, truck platoons may improve the situation for themselves as well, leading to potentially less delay, smoother speed profiles, as well as increased predictability.

To this end, we need an appropriate model of the mutual influence that truck platoons and the rest of the traffic have on each other, that is both tractable and sufficiently rich. Microscopic traffic models allow for a fairly straightforward representation of trucks and platoons [22], and PDE models offer a consistent way of introducing moving bottlenecks [23], but both are overly complex and detailed for link-level control synthesis. The multi-class cell transmission model (CTM) [24] presents a good balance of complexity and tractability, and will therefore be used as a simulation model in this work. We further simplify this model using a queuing representation, and use it for control design.

The problem that we are addressing in this paper is bottleneck decongestion using randomly arriving platoons as actuators, using their speed and the number of lanes they occupy as a control input. The main contributions of this work are the queuing-based model for predicting the evolution of the traffic, and the control law that uses this prediction to improve the throughput. The designed control law is tested on a road segment upstream of a lane drop bottleneck that has one on-ramp and one off-ramp, and shown to achieve a significant reduction in total time spent. The median delay of all vehicles was reduced 75.6% in case the proposed control was applied, compared to the case with no control. Even though the platoons are slowed down while actuating control actions, they experience overall less delay compared to the case without control, since they avoid going through congestion at the bottleneck.

The paper is structured as follows. In Section 2, we present the multi-class CTM and introduce its simplified queuing representation. Then, in Section 3, we use the said simplified model to design control laws for improving the throughput of the road. Next, in Section 4, we describe the simulation setup and results, and finally, in Section 5 we conclude and discuss the results.

2 MODELING

In this section, we present the traffic models that will be used for analysis, simulation and control design. An example of the highway segment, similar to the one we model, is shown in Figure 1. The base model, multi-class CTM, is augmented to properly represent the behavior of platoons moving slower than the rest of traffic. Since this model still has a high number of states and control inputs, we propose a simplified queuing model, that is consistent with the multi-class CTM, and use it for control design. Control actions will be calculated using predictions based on this simplified model, and then applied to the more complex simulation model for evaluations.

2.1 The multi-class CTM

The simulation model that is used in this work is a multi-class extension of the well-known CTM [25], and it is a variant of the model used in [26] and [24]. Let $\mathscr{K}$ be the set of vehicle classes. The traffic density of vehicles of class $\kappa \in \mathscr{K}$ in cell i at time t will be expressed in terms of passenger car equivalents, and denoted $\rho_i^\kappa(t)$. We allow each of the classes to have a distinct free flow speed $U_i^\kappa(t)$ in every cell, varying in time. In practice, we use $U_i^\kappa(t)$ to capture some richer behaviour not covered by the base model, like platoons stop-and-go waves, as well as to apply the control action to the classes of vehicles we have control over. We will use the platoon model given in [24] for simulation and control design.

Consider a highway stretch consisting of N cells. The evolution of cell traffic densities for each class is given by

$$\rho_i^\kappa(t+1) = \rho_i^\kappa(t) + \frac{T}{L_i}\left(q_{i-1}^\kappa(t) - q_i^\kappa(t) + r_i^\kappa(t) - s_i^\kappa(t)\right),$$

where $r_i^\kappa(t)$ is the inflow and $s_i^\kappa(t)$ the outflow of each vehicle class from a potential on-ramp and to a potential off-ramp, respectively. The traffic flow of each class from cell i to cell $i+1$ is given by

$$q_i^\kappa(t) = \min\left\{D_i^\kappa(t), S_{i+1}^\kappa(t)\right\}.$$

The demand and supply functions of each class $D_i^\kappa(t)$ and $S_i^\kappa(t)$ also depend on vehicles of other classes. We write the demand and supply functions

$$\begin{aligned} D_i^\kappa(t) &= U_i^\kappa(t)\rho_i^\kappa(t)\min\left\{1, \frac{Q_i^{\max}}{\sum\limits_{k\in\mathscr{K}} U_i^k(t)\rho_i^k(t)}\right\}, \\ S_i^\kappa(t) &= \frac{\rho_{i-1}^\kappa(t)}{\rho_{i-1}(t)}\min\left\{W_i(P_i-\rho_i(t)), Q_i^{\max}, F_{i-1}(t)\right\}. \end{aligned}$$

Here, cell parameters L_i, V_i, W_i, σ_i and P_i are the length, free flow speed, congestion wave speed, critical density and jam density of cell i, respectively, and $Q_i^{\max} = V_i\sigma_i$. Function $F_{i-1}(t)$ models the capacity drop, and $\rho_i(t) = \sum_{\kappa\in\mathscr{K}}\rho_i^\kappa(t)$ is the aggregate traffic density. Where not stated otherwise, the cell parameters will be equal for all cells, and $W = V\frac{\sigma}{P-\sigma}$, which yields a triangular fundamental diagram. The cell length L and time step T are taken so that $L = VT$.

We prioritize the mainstream flow and only accept on-ramp inflow that the road capacity can support, so a part of vehicles entering the road might have to queue at the on-ramp. We model the evolution of these queues $n_i^{r,\kappa}$, for on-ramps in cell i, with

$$\begin{aligned} n_i^{r,\kappa}(t) &= n_i^{r,\kappa} + (\bar{r}_i^\kappa(t) - r_i^\kappa(t))T, \\ r_i^\kappa(t) &= \begin{cases} \min\left\{D_{i,r}^\kappa(t), S_{i,r}^\kappa(t)\right\}, & \kappa\in\mathscr{K}\setminus\mathscr{K}^*, \\ \bar{r}_i^\kappa(t), & \kappa\in\mathscr{K}^*, \end{cases} \\ D_{i,r}^\kappa(t) &= \bar{r}_i^\kappa(t) + \frac{n_{r,j}^\kappa(t-1)}{T}, \\ S_{i,r}^{r,\kappa}(t) &= \frac{n_i^{r,\kappa}(t)}{\sum\limits_{m\in\mathscr{K}\setminus\mathscr{K}^*} n_i^{r,m}(t)}\max\left\{0, \min\left\{S_i(t)-D_i(t), 0\right\} - \sum_{m\in\mathscr{K}^*} r_i^m(t)\right\}. \end{aligned}$$

Here, $\bar{r}_i^\kappa(t)$ is the total flow of vehicles arriving at the on-ramp, $S_i(t)$ and $D_i(t)$ are the aggregate supply and demand of cell i, and $\mathscr{K}^*$ is the set of prioritized traffic classes. Vehicles of class $\kappa\in\mathscr{K}^*$ do not queue at the on-ramps, and instead enter the road directly.

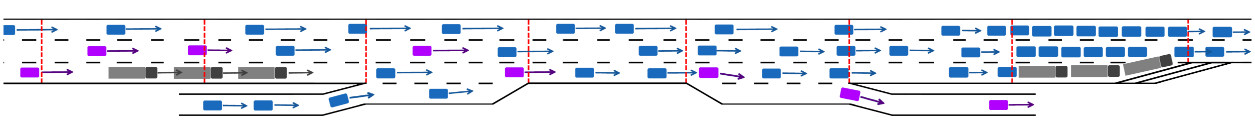

FIGURE 1 : Representation of the road segment with one on-ramp, one off-ramp, and a lane drop bottleneck that is considered in this work. Blue vehicles and truck platoons are mainstream-bound, whereas purple vehicles are off-ramp-bound. Dashed red line indicates cell boundaries

One of the benefits of multi-class CTM is that it can exactly define the flow to off-ramps, by representing vehicles with different destinations with different classes. Let i be a cell with an off-ramp where vehicles of classes $\mathscr{K}_i^r \subset \mathscr{K}$ exit the mainstream. We may then write

$$s_i^\kappa(t) = \begin{cases} \min\left\{D_i^\kappa(t), S_{i+1}^\kappa(t), S_{r,i}^\kappa(t)\right\}, & \kappa \in \mathscr{K}_i^r, \\ 0, & \kappa \notin \mathscr{K}_i^r, \end{cases}$$
$$S_{r,i}^\kappa(t) = \frac{\rho_i^\kappa}{\sum\limits_{m \in \mathscr{K}_i^r} \rho_i^\kappa(t)} Q_{r,i}^{\max},$$

where $Q_{r,i}^{\max}$ is the capacity of the off-ramp. Finally, we update $q_i^\kappa(t)$ accordingly,

$$q_i^\kappa(t) = \begin{cases} \min\left\{D_i^\kappa(t), S_{i+1}^\kappa(t)\right\}, & \kappa \notin \mathscr{K}_i^r, \\ 0, & \kappa \in \mathscr{K}_i^r. \end{cases}$$

Out of many ways of modeling capacity drop in first-order traffic models [27], we chose to capture it as a linear reduction of capacity, as in [28]. Denoting by α the maximum capacity drop ratio under jam traffic density, we have

$$F_i(t) = \min\left\{W_i \frac{\sigma_{i+1}}{\sigma_i}\left(P_i - (1-\alpha)\sigma_i - \alpha\rho_i(t)\right), Q_i^{\max}\right\}.$$

Note that because of this phenomenon, the actual speed of the congestion wave will be different than W.

In our case, vehicles of class a will represent platooned vehicles. Let there be Π platoons, and let platoon p move at speed $u_p(t) \in [U_{\min}, U_{\max}]$, with $U_{\max} < V$. We denote the position of the platoon head (downstream end) $x_p(t)$, $x_1(t) > x_2(t) > \cdots > x_\Pi(t)$, and the reference density of platooned vehicles $\rho_p(t)$. Assuming the length of the platoon is $l_p \geq 2L$, the traffic density profile in the cells that contain it is

$$\rho_i^a(t) = \begin{cases} 0, & i < i_\Pi^t(t), \\ \rho_p(t) \frac{X_{i_p^t(t)+1} - x_p(t) + l_p}{L}, & i = i_p^t(t), p = 1, \ldots \Pi, \\ \rho_p(t), & i_p^t(t) < i < i_p^h(t), p = 1, \ldots \Pi, \\ \rho_p(t) \frac{x_p(t) - X_{i_p^h(t)}}{L}, & i = i_p^h(t), p = 1, \ldots \Pi, \\ 0, & i_p^h(t) < i < i_{p-1}^t(t), p = 1, \ldots \Pi, \end{cases} \tag{1}$$

where $i_p^h(t) = \lceil x_p(t)/L \rceil$ and $i_p^t(t) = \lceil (x_p(t) - l_p)/L \rceil$ are the cells in which the platoon head and tail (downstream and upstream end) are, and $i_0^t = N$. The platoon position updates after T will be $x_p(t+1) = x_p(t) + u_p(t)T$, and class a traffic densities need to be updated accordingly, which is achieved by setting

$$U_i^a(t) = \begin{cases} V, & i < i_\Pi(t)^t, \\ \frac{V}{\rho_i^a(t)} \left(\rho_p(t) - \frac{V - U_{i+1}^a(t)}{V} \rho_{i+1}^a(t) \right), & i_p^t(t) \leq i < i_p^h(t), p = 1, \dots, \Pi, \\ V - (V - u_p(t)) \frac{\rho_p(t)}{\rho_i^a(t)}, & i = i_p^h(t), p = 1, \dots, \Pi, \\ 0, & i_p^h(t) < i < \frac{i_p^h(t) + i_{p-1}^t(t)}{2}, p = 1, \dots, \Pi, \\ V, & \frac{i_p^h(t) + i_{p-1}^t(t)}{2} \leq i < i_{p-1}^t(t), p = 1, \dots, \Pi. \end{cases} \tag{2}$$

Even if the initial class a density profile differs from the reference, by applying (2) it will converge to (1). Furthermore, the traffic flow overtaking a platoon with density ρ_p will be $V(\sigma - \rho_p)$, which is consistent with PDE moving bottleneck models.

Consider a bottleneck at the location of a lane drop, from n_-^l to n_+^l lanes, $n_+^l < n_-^l$. This corresponds to going from a segment with critical density $\sigma_- = n_-^l \sigma^l$ to $\sigma_+ = n_+^l \sigma^l$, and the capacity of such bottleneck is $q_b^{max} = V\sigma_+$. However, due to the capacity drop phenomenon, in case of excess demand at the bottleneck, its capacity will be decreased once it becomes congested. A congestion of density ρ_c will be formed, with the density of discharging traffic being ρ_d. The congestion density ρ_c can be calculated from $W(P_- - \rho_c) = W\frac{\sigma_+}{\sigma_-}(P_- - (1-\alpha)\sigma_- - \alpha\rho_c)$,

$$\rho_c = \frac{P_-(\sigma_- - \sigma_+) + (1-\alpha)\sigma_-\sigma_+}{\sigma_- - \alpha\sigma_+},$$

and we calculate the discharge density from $V\rho_d = W(P_- - \rho_c)$,

$$\rho_d = \frac{\sigma_-\sigma_+(1-\alpha)}{\sigma_- - \alpha\sigma_+} < \sigma_+. \tag{3}$$

Since the outflow from the bottleneck is reduced to $q_d = V\rho_d < V\sigma_+$, arriving vehicles will have to wait and their total travel time increase. We will use the *Total Time Spent* (TTS), which is the sum of the total time all vehicles spent on the road and the time all vehicles spent queuing at on-ramps, as the performance index of the system,

$$\text{TTS} = \sum_{t=1}^{t_{end}} \sum_{\kappa \in \mathscr{K}} \sum_{i=1}^{N} \left(\rho_i^\kappa(t) L + n_i^{r,\kappa}(t) \right) T.$$

In order to minimize the TTS, we need to keep the demand at the bottleneck as high as possible, while keeping the bottleneck in free flow.

The multi-class CTM described in this section can describe fairly complex phenomena, but in order to do this and have a good spatial resolution of the results, we need to use very short cells, which makes simulation and prediction much less tractable. For example, if we want to model having platoons in traffic, that move at speeds different than V, we need the cell length L to be at most half of the platoon length. Therefore, L will be on the order of magnitude of tens of meters, so we will need a large number of cells to describe any longer highway stretch. This results in a system with $N|\mathscr{K}|$ states, where $|\mathscr{K}|$ is the number of vehicle classes, and up to $N|\mathscr{K}|$ control inputs if we assume that we can set separate free flow speeds $U_i^\kappa(t)$ for each class and each cell. In case we want to use this model to predict the outcome of applying some control action, e.g. as a part of optimization-based control, the problem will be intractable due to the large number of states.

However, we may exploit the specific form of the model and the problem to perform state space reduction without any approximations. Note that if the considered model is deterministic and $U_i^\kappa(t) = V$ for all classes and cells, assuming the highway was initially in free flow, the only place where we can expect congestion to emerge is at bottlenecks, where $Q_{i+1}^{\max} < Q_i^{\max}$. Elsewhere, if the road is in free flow, the future traffic density of a cell $\rho_i^\kappa(t+j)$ will be equal to the current traffic density of an upstream cell, $\rho_i^\kappa(t+j) = \rho_{i-j}^\kappa(t)$. Owing to this, we only need to know the initial traffic densities and follow what happens at the bottlenecks, i.e. how the length of their queues evolve in time, to have an accurate view of the full system. In the following section, we will derive such simplified model, that will then be used to calculate the appropriate control actions and close the loop.

2.2 Queuing model

In this work, we study the situation when there is a single bottleneck at the downstream end of the considered stretch of highway, and want predict its outflow based on the control action we chose for the platoons. Apart from this stationary bottleneck, platoons themselves can act as moving bottlenecks, since they will be moving slower than the rest of the traffic. We propose modeling this highway stretch using a queuing-based model, with queue length at the stationary bottleneck n_b and queue lengths at the platoons n_p, $p = 1, \ldots, \Pi$ as the only states. An example of a traffic situation with its corresponding queuing representation is shown in Figure 2.

Since this model is used for predicting the evolution of traffic after some time t_0, we assume that the current traffic situation $\rho_i^\kappa(t_0)$ is fully known and use this to predict the future values of system states. We enumerate the platoons that are on the considered highway segment at $t = t_0$, $p = 1, \ldots, \Pi$, and denote their position at that time x_p. In further text, we will assume that $t_0 = 0$, and that t represents the prediction time after t_0.

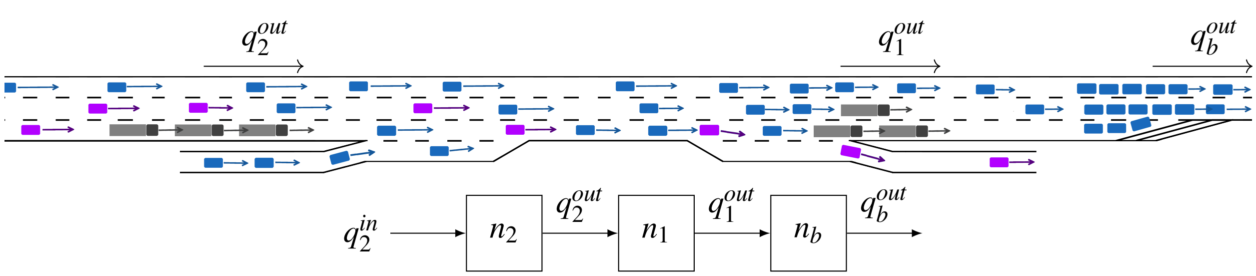

FIGURE 2 : Queues corresponding to static and moving bottlenecks. The static bottleneck corresponds to n_b, the downstream platoon to n_1 and the upstream platoon n_2. The overtaking flow of the downstream platoon q_1^{out} is limited to one lane of traffic, $q_1^{cap} = V\sigma_l$, and the overtaking flow of the upstream platoon q_2^{out} is limited to two lanes of traffic, $q_2^{cap} = V2\sigma_l$. Both the inflow from the on-ramp and the outflow to the off-ramp will factor in the inflow to the downstream platoon queue q_1^{in}.

The evolution of the queue at the bottleneck is given by

$$\dot{n}_b(t) = q_b^{in}(t) - q_b^{out}(t), \tag{4}$$

where the inflow and the outflow are

$$q_b^{in}(t) = q_b^u(t) + q_b^V(t), \tag{5}$$

$$q_b^{out}(t) = \begin{cases} q_b^{in}(t), & q_b^{in}(t) \leq q_b^{cap} \wedge n_b(t) = 0, \\ q_b^{dis}, & q_b^{in}(t) > q_b^{cap} \vee n_b(t) > 0. \end{cases} \tag{6}$$

Typically, due to capacity drop, the discharge rate of the queue at the bottleneck q_b^{dis} will be lower than its capacity q_b^{cap}, $q_b^{dis} < q_b^{cap}$. Mirroring the behaviour of the multi-class CTM, we set $q_b^{cap} = V\sigma_+ = Q_+^{\max}$ and $q_b^{dis} = V\rho_d$, according to (3). The inflow to the queue at the bottleneck $q_b^{in}(t)$ consists of two parts that travel at different speeds. The first part, $q_b^u(t)$, models the part of the demand that originates from the arrival of the platooned vehicles,

$$q_b^u(t) = \begin{cases} u_p\sigma_l, & t_p^u \leq t \leq t_p^u + \frac{l_p}{V}, \quad p = 1, \ldots, \Pi, \\ 0, & \text{otherwise}, , \end{cases} \tag{7}$$

$$t_p^u = \frac{X_b - x_p}{u_p},$$

where t_p^u represents the time at which platoon p reaches the bottleneck, and the second part consists of the background traffic travelling at free flow speed V,

$$q_b^V(t) = \begin{cases} q_p^{out}(\frac{x_p + Vt - X_b}{V - u_p}), & \max\left\{t_p^V, t_{p-1}^u\right\} \leq t \leq t_p^u, \quad p = 1, \ldots, \Pi, \\ V\rho(X_b - Vt), & \text{otherwise}, \end{cases}$$

$$t_p^V = \frac{X_b - x_p}{V}.$$

Here, the position of the bottleneck is $X_b = x_0$, and l_p is the length of platoon p. We assume that the platoon will approach the bottleneck taking up one lane, thus its density will be equal to the critical density per lane σ_l. The second part of the inflow $q_b^V(t)$ originates either from the initial traffic situation,

$$\rho(x) = \sum_{\kappa \in \mathcal{K} \setminus \mathcal{K}^\Pi} \rho_i^\kappa(0), \quad X_i \leq x < X_{i+1},$$

where $\mathcal{K} \setminus \mathcal{K}^\Pi$ is the set of all vehicle classes excluding the platooned vehicles class, or is the delayed overtaking flow of some platoon. Each platoon travels at its individual speed $u_p \leq V$, and we assume that this speed is constant during the prediction horizon. Furthermore, we assume that the platoon speeds are such that there is no platoon merging prior to reaching the bottleneck, $t_{p-1}^u > t_p^u$.

Under these assumptions, we define the evolution of the queue at each of the platoons as

$$\dot{n}_p(t) = \frac{V - u_p}{V}\left(q_p^{in}(t) - q_p^{out}(t)\right), \quad 0 \leq t \leq t_p^u,$$

for $p = 1,\dots,\Pi$. The evolution of queues is defined until time t_p^u, when the queue at the platoon is added to the queue at the bottleneck,

$$n_b(t_p^u+) = n_b(t_p^u) + n_p(t_p^u). \tag{8}$$

The outflow and inflow are defined the same way as with the bottleneck queue,

$$q_p^{out}(t) = \begin{cases} q_p^{in}(t), & q_p^{in}(t) \le q_p^{cap}(t) \wedge n_p(t) = 0, \\ q_p^{dis}(t), & q_p^{in}(t) > q_p^{cap}(t) \vee n_p(t) > 0, \end{cases}$$
$$q_p^{in}(t) = \begin{cases} q_{p+1}^{out}\left(\frac{(V-u_p)t - x_p + x_{p+1}}{V-u_{p+1}}\right), & t > \frac{x_p - x_{p+1}}{V-u_p}, \\ V\rho(x_p - (V-u_p)t, 0), & t \le \frac{x_p - x_{p+1}}{V-u_p}, \end{cases}$$

except here we assume $q_p^{dis}(t) = q_p^{cap}(t)$, and allow $q_p^{cap}(t)$ to vary in time and be used as a control input. Since the considered road stretch has three lanes, we assume here that platoons can either take one lane or two lanes. In case platoon p is taking one lane at time t, we set $q_p^{cap}(t) = V(\sigma_- - \sigma_l$, and if it is taking two lanes, $q_p^{cap}(t) = V(\sigma_- - 2\sigma_l)$.

The model can be simplified by adopting a coordinate transfer $\tau_p = \frac{x_p - X_b + Vt}{V-u_p}$, $t = \frac{V-u_p}{V}\tau_p + \frac{X_b - x_p}{V}$, for each platoon, which yields

$$\frac{\mathrm{d}n_p(t(\tau_p))}{\mathrm{d}\tau_p} = q_p^{in}(t(\tau_p)) - q_p^{out}(t(\tau_p)), \quad t_p^V \le \tau_p \le t_p^u$$

and, taking $\tilde{n}_p(\tau_p) = n_p(t(\tau_p))$, $\tilde{q}_p^{in}(\tau_p) = q_p^{in}(t(\tau_p))$, and $\tilde{q}_p^{out}(\tau_p) = q_p^{out}(t(\tau_p))$, we may write

$$\dot{\tilde{n}}_p(t) = \tilde{q}_p^{in}(t) - \tilde{q}_p^{out}(t), \quad t_p^V \le t \le t_p^u \tag{9}$$

for each $p = 1,\dots,\Pi$. The inflow to the queue at the bottleneck and at platoons can now be simplified to

$$q_b^V(t) = \begin{cases} \tilde{q}_p^{out}(t), & \max\left\{t_p^V, t_{p-1}^u\right\} \le t \le t_p^u, \\ V\rho(X_b - Vt), & \text{otherwise}, \end{cases}$$
$$\tilde{q}_p^{in}(t) = \begin{cases} \tilde{q}_{p+1}^{out}(t), & t_{p+1}^V < t < t_{p+1}^V, \\ V\rho(X_b - Vt, 0), & t \le t_{p+1}^V, \end{cases}$$

and the outflow from the platoon becomes

$$\tilde{q}_p^{out}(t) = \begin{cases} \tilde{q}_p^{in}(t), & \tilde{q}_p^{in}(t) \le \tilde{q}_p^{cap}(t) \wedge \tilde{n}_p(t) = 0, \\ \tilde{q}_p^{cap}(t), & \tilde{q}_p^{in}(t) > \tilde{q}_p^{cap}(t) \vee \tilde{n}_p(t) > 0, \end{cases} \tag{10}$$

In case there are on- and off-ramps, their influence can be added to $q_b^V(t)$ and $\tilde{q}_p^{in}(t)$. Denoting $q_k^r(t)$ the inflow from an on-ramp (if $q_k^r(t) \ge 0$), or outflow to an off-ramp (if $q_k^r(t) \le 0$), we may write

$$q_b^V(t) = q_b^{V\setminus r}(t) + \sum_{k\in K_o^d(t)} \tilde{q}_k^r(t), \tag{11}$$
$$q_b^{V\setminus r}(t) = \begin{cases} \tilde{q}_p^{out}(t), & \max\left\{t_p^V, t_{p-1}^u\right\} \le t \le t_p^u, \\ V\rho(X_b - Vt), & \text{otherwise}, \end{cases}$$
$$K_o^d(t) = \begin{cases} K_p^b(t), & \max\left\{t_p^V, t_{p-1}^u\right\} \le t \le t_p^u, \\ K_\rho^b(t), & \text{otherwise}. \end{cases}$$

For the inflow to the queue at platoons, we write

$$\tilde{q}_p^{in}(t) = \tilde{q}_p^{in\setminus r}(t) + \sum_{k\in K_o^d(t)} \tilde{q}_k^r(t), \tag{12}$$
$$\tilde{q}_p^{in\setminus r}(t) = \begin{cases} \tilde{q}_{p+1}^{out}(t), & t > t_{p+1}^V, \\ V\rho(X_b - Vt), & t \le t_{p+1}^V, \end{cases}$$
$$K_o^d(t) = \begin{cases} K_{p+1}^p(t), & t > t_{p+1}^V, \\ K_\rho^p(t), & t \le t_{p+1}^V. \end{cases}$$

Here, $\tilde{q}_k^r(t) = q_k^r(t - \frac{X_b - X_k^r}{V})$, and $K_o^d(t)$ are sets of indices of all on- and off-ramps with positions $X_k^r < X_b$ between the bottleneck or platoon p, and the place where their inflows would originate from,

$$K_p^b(t) = \left\{k \,\middle|\, x_p^u(t) < X_k^r \le X_b, t \ge t_k^r \right\},$$
$$K_\rho^b(t) = \left\{k \,|\, X_b - Vt < X_k^r \le X_b, t \ge t_k^r \right\},$$
$$K_{p+1}^p(t) = \left\{k \,\middle|\, x_{p+1}^u(t) < X_k^r \le x_p^u(t), t \ge t_k^r \right\},$$
$$K_\rho^p(t) = \left\{k \,\middle|\, X_b - Vt < X_k^r \le x_p^u(t), t \ge t_k^r \right\},$$
$$t_k^r = \frac{X_b - X_k^r}{V},$$

and we define $x_p^u(t)$ as

$$x_p^u(t) = \frac{u_p V t + V x_p - u_p x_p}{V - u_p}.$$

Note that $q_k^r(t)$ will depend on the local traffic conditions around X_k^r at time t. Furthermore, since a portion of the queue at the platoon will also leave the road via the off-ramp, we reduce $\tilde{n}_p$ at the time when the platoon reaches it,

$$\tilde{n}_p(t+) = \tilde{n}_p(t) - \Delta_p^{r,k}(t), \quad x_p^u(t) = X_k^r, \tag{13}$$

and the part of the queue $\tilde{n}_p(t)$ that leaves the highway, $\Delta_p^{r,k}(t)$, depends on the ratio of off-ramp-bound vehicles in the platoon queue.

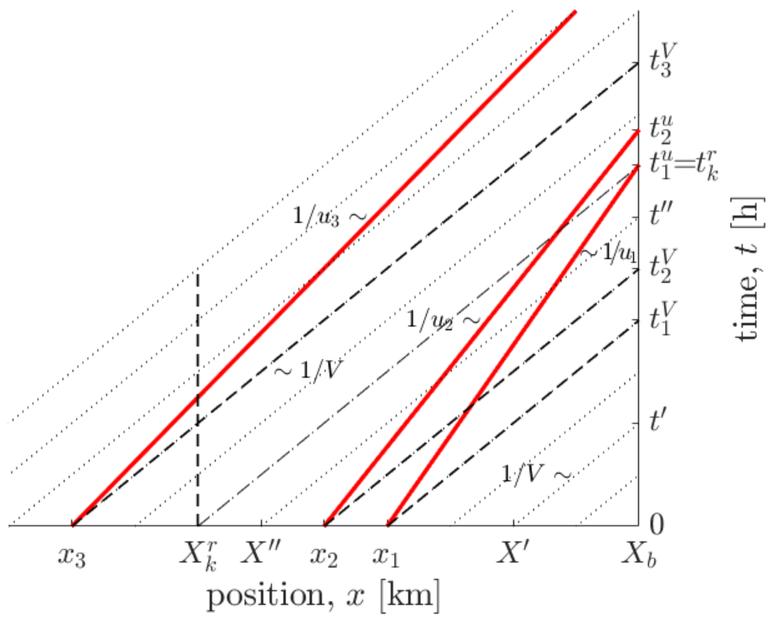

FIGURE 3 : Illustration of the queuing model. The dotted lines represent free flow propagation. Platoon trajectories are shown in red. As shown in the figure, at time t', inflow to the bottleneck is $q_b^{in}(t') = V\rho(X')$. At time t'', inflow to the bottleneck is $q_b^{in}(t'') = \tilde{q}_1^{out}(t'')$, and inflows to the platoons $q_1^{in}(t'') = \tilde{q}_2^{out}(t'')$, and $q_2^{in}(t'') = V\rho(t'')$. Ramp k will affect $q_2^{in}(t)$ for $t_k^r < t \leq t_2^u$, $q_3^{in}(t)$ while $x_3^u(t) \geq X_k^r$ and $t < t_3^u$, and $q_b^{in}(t)$ the rest of time.

Finally, an illustration of the derivation of the proposed model is given in Figure 3. In summary, the proposed model consists of $\Pi + 1$ states, whose evolution is described by (4) and (9). Inflow to the bottleneck is given by (5), and consists of the background traffic travelling at free flow speed (11), and the platoons (7). Outflow from the bottleneck is (6), and there are discontinuous jumps in this state triggered by the arrival of platoons at the bottleneck, (8). For each platoon queue, inflow is given by (12), outflow by (10), and there is a discontinuous jump in the state when the platoon passes an off-ramp, (13). The model can be described as a tandem queuing system, with saturation and hysteresis, time-varying structure and jumps.

3 CONTROL

Having defined the simplified model of the system, in this section we will formulate a control law for improving the throughput of the system. In general, the control objective we consider can be formulated as shaping the traffic flow at some position. We are looking to maximize the outflow from the bottleneck, which in case there are no off-ramps corresponds to minimizing the total travel time. In case there are off-ramps the total outflow of the mainstream and of the off-ramps needs to be maximized instead. We first consider the case when there are no on- or off-ramps and then extend the control to include on- and off-ramps.

3.1 Ideal actuation

In order to have a baseline for comparing the performance of our proposed control laws, we first consider the ideal case, assuming we can fully control all traffic, and that we can control every class of traffic independently. This corresponds to having a 100% penetration rate of connected, communicating, and controlled vehicles, and knowing each vehicle's destination. Since we already assumed that the demand of off-ramp-bound vehicles is lower than the capacity of the off-ramp, we only need to minimally delay the mainstream-bound background traffic so that the demand at the bottleneck never exceeds its capacity. This is equivalent to ensuring that the traffic density immediately upstream of the bottleneck $\rho_{i_b}(t) \leq \sigma_+$ for all t, and can be achieved by setting

$$
\begin{aligned}
&U_{i_b}^b(t) = V,\\
&U_i^b(t) = \min\left\{V, \max\left\{U_{\min}^b, \frac{V}{\rho_i^b(t)}\left(\rho_i^{b,ref}(t) - \frac{V - U_{i+1}^b(t)}{V}\rho_{i+1}^b(t)\right)\right\}\right\}, \quad i = 1, \dots, i_b - 1
\end{aligned}
$$

$$
\rho_i^{b,ref}(t) = \begin{cases} \sigma_+ - \rho_p, & \frac{X_b - x_p(t)}{u_p(t)} < \frac{X_b - X_i}{V} < \frac{X_b - x_p(t) + l_p(t)}{u_p(t)} + \frac{L}{V}, \quad p = 1, \dots, \Pi, \\ \sigma_+, & \text{otherwise.} \end{cases}
$$

This way, the mainstream-bound background traffic is regulated so that the total demand at the bottleneck, including the arriving platoons, is kept as close to its capacity as possible without exceeding it. The mainstream-bound background traffic is delayed minimally, while the platoons and the off-ramp-bound background traffic travel at their respective maximum speeds.

3.2 Platoon-actuation not aware of on- or off-ramps

The control objective, maximizing the throughput, i.e. the outflow q_b^{out}, can be achieved by keeping $n_b = 0$ and $q_b^{in} = q_b^{cap}$. Additionally, we require that the queue at the platoon is already discharged when the platoon reaches the bottleneck, $n_p(t_p^u) = 0$. Therefore we may employ control law

$$
\tilde{q}_p^{cap}(t) = \begin{cases} q^{ref}(t), & n_b(t) = 0 \wedge t \geq t_{p-1}^u, \\ \tilde{q}_{p-1}^{cap}(t), & \tilde{n}_{p-1}(t) = 0 \wedge t < t_{p-1}^u, \\ Q^{lo}, & \text{otherwise,} \end{cases} \tag{14}
$$

where the reference flow $q^{ref}(t)$ can be externally determined. For maximizing the throughput, we set

$$
q^{ref}(t) = Q^{hi} - q_b^u(t),
$$

taking the largest admissible $Q^{hi} \leq q_b^{cap}$. In order to compute the current $q_p^{cap}(t) = \tilde{q}_p^{cap}(t_p^V)$ for all platoons, we need to predict n_b until t_Π^V, which requires calculating $q_\Pi^{cap}(0)$ and $q_p^{cap}(t)$ for $0 \leq t \leq \min\left\{t_p^u, t_\Pi^V\right\}$.

Assuming this control law is applied, we may calculate the speed of each platoon so that $n_p(t_p^u) = 0$ and $n_b(t) = 0, t_p^c \leq t \leq t_p^u$, with minimum t_p^c, and

$$
t_p^c \geq \max\left\{t_p^V, t_{p-1}^{u_{p-1}} + \frac{l_{p-1}}{V}\right\}.
$$

This is achieved when

$$\tilde{n}_p(t_p^u) = \tilde{n}_p(t_p^c) + \int_{t_p^c}^{t_1^u} \tilde{q}_1^{in}(t)\mathrm{d}t - Q^{hi}(t_1^u - t_1^c) = 0. \tag{15}$$

For $p = 1$, in case it is known that $t_2^V < t_1^u$, (15) simplifies to

$$\begin{aligned}\tilde{n}_1(t_1^u) &= \tilde{n}_1(t_2^V) + Q^{lo}(t_1^u - t_1^c) - Q^{hi}(t_1^u - t_1^c) = 0,\\ u_1 &= \frac{\left(Q^{hi} - Q^{lo}\right)(X_b - x_1)}{\tilde{n}_1(t_2^V) + \left(Q^{hi} - Q^{lo}\right) t_1^c},\end{aligned}$$

since we can explicitly calculate $\tilde{n}_1(t_2^V) = \int_{t_1^V}^{t_2^V} V\rho(X_b - Vt, 0)\mathrm{d}t - Q^{lo}(t_2^V - t_1^V)$. Otherwise, u_p is calculated by solving (15) numerically, and can be obtained as a by-product of iterating the prediction steps for n_b and $\tilde{n}_p$. The simplest way of calculating u_p is to initialize it to

$$\min\left\{U_{\max}, u_{p-1}\frac{X_b - x_p}{X_b - x_{p-1} + l_{p-1}}\right\},$$

and then decrease it until either $u_p = U_{\min}$ or (15) is satisfied. This also ensures that u_p is constrained to be within the range

$$U_{\min} \leq u_p \leq \min\left\{U_{\max}, u_{p-1}\frac{X_b - x_p}{X_b - x_{p-1} + l_{p-1}}\right\},$$

which is required for the limitations to be met if there is no platoon merging.

3.3 Platoon-actuation aware of on- or off-ramps

Consider now the case when there are on- or off-ramps. In order to predict the evolution of queues, which is needed for calculating the control inputs, we need to know the ramp flows $\tilde{q}_k^r(t)$ in advance. This information can be hard to obtain, since it will depend on the routing decisions of individual drivers constituting the background traffic. Therefore, we use the predicted ramp flows.

If ramp k is an on-ramps, we can replace the actual ramp flow with its average $\hat{q}_k^r = \bar{q}_k^r$, which in reality can be determined statistically. If ramp k is an off-ramp, we can employ the standard assumption that some constant ratio of vehicles R_k leave the road via the off-ramp. We can then write

$$\begin{aligned}\hat{q}_k^r(t) &= -R_k\left(\tilde{q}_k^{in,r}(t) + \sum_{l\in K_o^{k,r}(t)} \tilde{q}_l^r(t)\right),\\ \tilde{q}_k^{in,r}(t) &= \begin{cases} q_b^V(t), & x_1^u(t) < x_k^r < X_b\\ \tilde{q}_{p+1}^{out}(t), & x_{p+1}^u(t) < x_k^r < x_p^u(t)\end{cases}\\ K_o^{k,r}(t) &= \begin{cases}\left\{l | x_p^u(t) < x_l^r < x_k^r\right\}, & t > t_p^V, p = 1 \vee x_k^r < x_{p-1}^u(t)\\ \left\{l | X_b - Vt < x_l^r < x_k^r\right\}, & \text{otherwise}\end{cases}\end{aligned}$$

depending on where the flow to off-ramp k at time t originates from.

The portion of queue at platoon p that leaves the highway at off-ramp k can be estimated to be

$$\tilde{n}_p(t+) = (1 - R_k)\tilde{n}_p(t), \quad x_p^u(t) = x_k^r,$$

and we may now apply a control law similar to the one derived for the case when there are no on- and off-ramps, (14). We modify (14) to take into account the fact that there might be some off-ramps $k \in K^*$ whose flow we do not want to obstruct. Since it is not possible to selectively allow the off-ramp-bound traffic to pass without also releasing the mainstream-bound traffic, we will only allow unrestricted flow towards those off-ramps by setting $\tilde{q}_p^{cap} = Q^{hi}$ if there are other platoons downstream that are regulating the inflow to the bottleneck. The updated control law is

$$\tilde{q}_p^{cap}(t) = \begin{cases} q^{ref}(t), & n_b(t) = 0 \wedge t \geq t_{p-1}^u, \\ Q^{hi}, & K_p^{p-1}(t) \cap K^* \neq \emptyset \wedge t < t_{p-1}^u, \\ \tilde{q}_{p-1}^{cap}(t), & K_p^{p-1}(t) \cap K^* = \emptyset \wedge \tilde{n}_{p-1}(t) = 0 \wedge t < t_{p-1}^u, \\ Q^{lo}, & \text{otherwise.} \end{cases}$$

The platoon speeds are again obtained in the course of calculating the queue evolution predictions, as described in the previous subsection.

4 SIMULATION-BASED VALIDATION

In order to assess the performance of proposed control laws, we conducted a number of simulation runs, results of which will be presented in this section.

The simulations were executed on a 5 km long stretch of highway, with an on-ramp around the 2 km mark, and an off-ramp around the 3 km mark. Most of the highway stretch has three lanes, corresponding to a critical density of $\sigma_- = 60$ veh/km and capacity of $Q_-^{\max} = 6000$ veh/h, with free flow speed of $V = 100$ km/h. There is a bottleneck caused by a lane drop 80 m upstream of the end of the considered stretch, with capacity of $Q_+^{\max} = 4000$ veh/h. The capacity drop phenomenon is modelled with $\alpha = 0.4$, which causes the bottleneck capacity to be reduced to $Q_+^{dis} = 3273$ veh/h, representing a 18.2% capacity drop for this road configuration.

We considered three classes of traffic: class a consists of the platoons we control, class b is the mainstream-bound background traffic, and class c the off-ramp-bound background traffic. The arrival of class a vehicles is modelled as Poisson process with Poisson arrival rate of $\lambda = 81$ platoon/h. We assume that each platoon consists of 2 passenger car equivalents, although in reality, due to having shorter inter-vehicular gaps, these platoons might be up to about five passenger cars or about three trucks long. This effect was not included in calculating the TTS, and including it would only further emphasize the benefits of proposed control. The inflow of background traffic is assumed to be time-varying and uniformly distributed, changing every 14.4 seconds. At the beginning of the highway segment, the demand of mainstream-bound background traffic takes values in $\bar{r}_1^b(t) \sim \mathscr{U}(1000, 2000)$ veh/h, and the demand of off-ramp bound traffic is $\bar{r}_1^c(t) \sim \mathscr{U}(750, 1250)$ veh/h. Since the on-ramp and off-ramp are reasonably close, we assume that none of the vehicles entering the highway via the on-ramp will exit it via the off-ramp, $\bar{r}_{i_{on}}^c(t) = 0$ veh/h. The demand of mainstream-bound traffic at the on-ramp is modelled as $\bar{r}_{i_{on}}^b(t) \sim \mathscr{U}(900, 1500)$ veh/h.

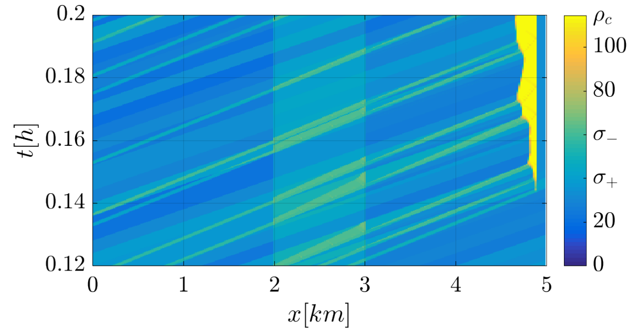

(a) No control

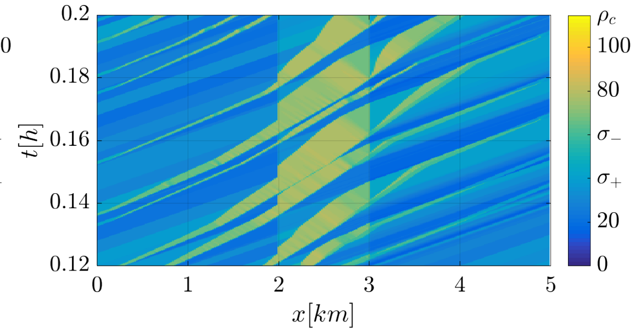

(b) Platoon-actuated control ignoring on- and off-ramps

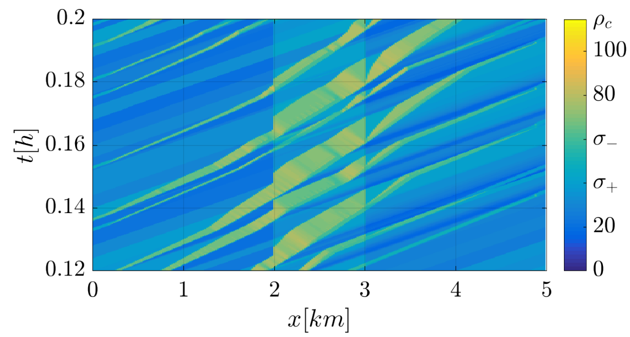

(c) Platoon-actuated control taking on- and off-ramps into account

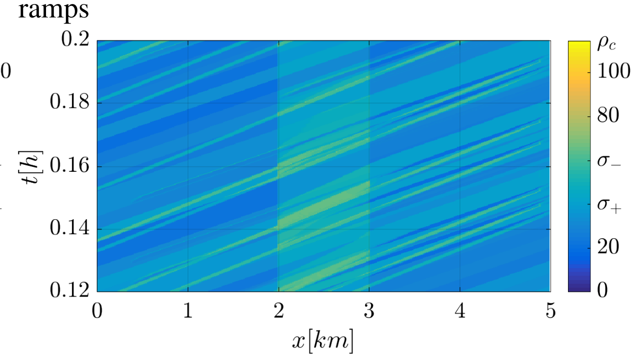

(d) Ideally actuated control

FIGURE 4 : An example comparing the outcome of the four simulation cases. Traffic density is color-coded, with warmer color representing higher density.

The duration of each simulation run is 2 hours, of which the background traffic inflow is halved for the first 3 minutes, in order to properly initialize the system, and for the last 12 minutes, in order to allow the traffic to return to free flow and ensure fair comparison between different control laws. Simulations are done with four cases of control:

(a) No control
(b) Platoon-actuated control ignoring on- and off-ramps
(c) Platoon-actuated control taking on- and off-ramps into account
(d) Ideally actuated control

In order to demonstrate the effect applying these control laws has on the traffic, a part of one simulation run is shown in Figure 4.

Consider the uncontrolled case shown in Figure 4a. Around time $t = 0.144$ h, the aggregate density of the platooned vehicles and background traffic arriving at the bottleneck is too high, and the aggregate demand exceeds bottleneck capacity. This causes a traffic breakdown, and after a brief transient, congestion is formed and bottleneck capacity is reduced. Because of this, even though the incoming traffic density is lower after $t = 0.154$ h, and would not exceed the original bottleneck capacity, it is not enough to dissipate the congestion at the bottleneck. Consequently, the throughput is reduced, the total time spent significantly increased, and the bottleneck will stay congested until the inflow to the highway segment is reduced close to the end of the simulation run.

In contrast to this, in the ideally actuated case shown in Figure 4d, a part of the mainstream-bound background traffic is delayed so that the density of other vehicles reaching the bottleneck while a platoon is traversing it is low enough so as not to cause traffic breakdown and capacity drop. In this way, free flow is maintained and throughput is close to its theoretical maximum.

As shown in Figure 4b and Figure 4c, the performance of the two proposed control laws is similar. However, in case the influence of on- and off-ramps is ignored while predicting the evolution of the system, the applied control action is more severe than required, which leads to more congestion upstream of the off-ramp and overall lower efficiency. The control law that takes the on- and off-ramps into account comes close to emulating the ideal actuation case, but achieves somewhat worse performance because it is unable to selectively affect only one class of background traffic, only has access to the average splitting ratio for the off-ramp, and requires delaying the platoons.

We executed 50 simulation runs for each control case, with the same platoon arrival times and background traffic inflow profiles. The resulting average and median TTS are shown in Table 1. We show the TTS of each vehicle class, and for all vehicles combined. Apart from comparing the TTS, we also considered the delay, defined as the difference in TTS compared to the ideal actuation case, which is taken as a benchmark for minimum achievable TTS of each simulation run. The delay is shown as percentage of minimum travel time, and it is shown as a box plot in Figure 5, and given in Table 2. For example, if a vehicle would traverse the road segment in 3 minutes if it travelled at free flow speed, and actually traverses it in 4.5 minutes, we say that it had a 50% delay.

We can see that even by applying control that ignores the existence of on- and off-ramps, as described in Section 3.2, we reduce the TTS by about 10% of the ideal TTS on average, with the median reduced by about 17%. This corresponds to eliminating 29.1% of the delay on average, or 43.7% by median. However, only the TTS of class b, the mainstream-bound background traffic, is reduced, while the TTS of other vehicles is even somewhat increased. This can be explained by the fact that the controller assumes that all vehicles are headed for the bottleneck, and will therefore delay the traffic too much, stalling the off-ramp-bound traffic which would otherwise be able to leave the highway unhindered. In spite of this inefficiency, and owing to the fact that vehicles of class b comprise the majority of the traffic, this control law is still able to preserve free flow and forestall capacity drop at the bottleneck, thus the overall TTS and delays are lower than in the uncontrolled case.

In contrast, when the control from Section 3.3 was used, the TTS of both class a (the platooned

TABLE 1 : Average and median TTS for each vehicle class and all vehicles.

TTS	Class a		Class b		Class c		Total	
[veh h]	average	median	average	median	average	median	average	median
Case (a)	22.62	22.94	369.84	374.13	56.62	56.04	449.08	453.94
Case (b)	23.25	23.03	329.91	315.75	60.62	60.37	413.78	398.18
Case (c)	21.77	21.34	304.90	278.63	58.60	58.41	385.27	357.58
Case (d)	17.00	16.91	255.00	254.09	55.92	55.93	327.92	326.42

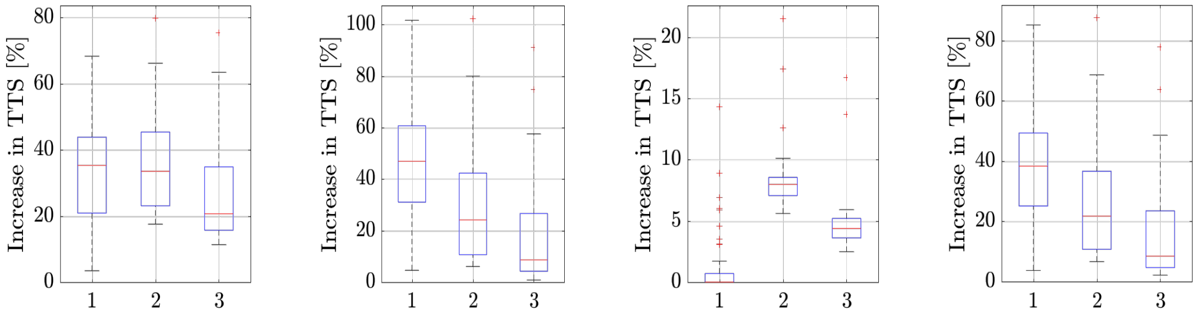

FIGURE 5 : Box plots showing the increase in TTS compared to the ideal actuation case.

TABLE 2 : Average and median delay for individual vehicle classes and all vehicles.

Delay [%]	Class a		Class b		Class c		Total	
	average	median	average	median	average	median	average	median
Case (a)	33.1	35.3	45.0	46.9	1.2	0.0	36.9	38.3
Case (b)	36.8	33.5	29.4	24.1	8.4	8.0	26.2	21.7
Case (c)	28.1	20.7	19.6	8.6	4.8	4.4	17.5	8.4

vehicles) and class b vehicles, is reduced, with the aggregate TTS lower by almost 20% of ideal TTS on average, or by almost 30% in median. This corresponds to eliminating 52.7% of the delay on average, or 75.6% by median. Even though the platoons will be delayed in order to actuate the control action, their TTS will be lower, since they will avoid waiting in congestion upstream of the bottleneck. This is especially important, since it shows that it is beneficial for the platooned vehicles to employ this control law, even if their goal is not to optimize the overall traffic performance, but to minimize only their own travel time. The TTS of class c vehicles is still increased compared to the uncontrolled case, but less so than with the previous control law. Overall, this control law comes very close to the ideal case, with the median delay being only 8.4%, and an average delay of 17.5%.

It is notable that while the proposed control laws achieve significant reduction of both average and median TTS, but there is a number of outliers corresponding to particularly unfavourable simulation runs. Since the arrival of platoons is modelled as a Poisson process, we can expect to occasionally have long gaps between two platoons. If this occurrence coincides with a higher demand of mainstream-bound background traffic, we will not be able to prevent the traffic breakdown, since there would be no platoons available to actuate the control action, resulting in a build-up of congestion and higher a TTS.

5 CONCLUSION

In this work, we use the multi-class CTM framework to study the effects of platoons arriving at a highway bottleneck. We propose a simplified queuing model that captures the important aspects of traffic dynamics, and use it to design control laws that use platoons as actuators, and their speed and depth as control inputs, to keep the bottleneck in free flow, maximizing throughput and minimizing total time spent of all vehicles. The performance of these control laws is tested in multi-class CTM simulations, on a 5 km long stretch of highway upstream of the lane drop bottleneck, going from three lanes to two. The considered highway segment also includes an on-ramp and an off-ramp. The achieved TTS using these control laws is compared to the case when no control is used, as well as with the case when we have ideal actuation, and can fully control all individual vehicles. It has been demonstrated that applying the proposed control laws significantly reduces the TTS compared to the situation with no control, coming close to the performance of the ideal actuation case. Moreover, even the platooned vehicles, which are delayed in order to affect the rest of traffic, incur lower delays, since they avoid having to traverse the congestion at the bottleneck, making the proposed control beneficial for all traffic participants.

For future work, we are interested in deriving theoretical bounds on effects of the proposed control laws in terms of total time spent and achievable throughput. Additionally, we plan to extend this work to handle longer highway sections, where multiple bottlenecks need to be regulated in cascade, as well as test the approach in microscopic traffic simulations. In general, the influence of truck platoons on the rest of traffic needs to be further investigated using both simulations and experiments on public roads.

ACKNOWLEDGMENTS

The research leading to these results has received funding from the European Union's Horizon 2020 research and innovation programme under the Marie Skłodowska-Curie grant agreement No 674875, NYU Tandon School of Engineering, the C2SMART University Transportation Center, VINNOVA within the FFI program under contract 2014-06200, the Swedish Research Council, the Swedish Foundation for Strategic Research, and Knut and Alice Wallenberg Foundation. The first author is affiliated with the Wallenberg AI, Autonomous Systems and Software Program (WASP).

REFERENCES

[1] Bergenhem, C., S. Shladover, E. Coelingh, C. Englund, and S. Tsugawa, Overview of platooning systems. In *Proceedings of the 19th ITS World Congress*, Vienna, Austria, 2012.

[2] Bonnet, C. and H. Fritz, *Fuel consumption reduction in a platoon: Experimental results with two electronically coupled trucks at close spacing*. SAE Technical Paper, 2000.

[3] Shladover, S., D. Su, and X.-Y. Lu, Impacts of cooperative adaptive cruise control on freeway traffic flow. *Transportation Research Record: Journal of the Transportation Research Board*, , No. 2324, 2012, pp. 63–70.

[4] Lioris, J., R. Pedarsani, F. Y. Tascikaraoglu, and P. Varaiya, Platoons of connected vehicles can double throughput in urban roads. *Transportation Research Part C: Emerging Technologies*, Vol. 77, 2017, pp. 292–305.

[5] Moridpour, S., E. Mazloumi, and M. Mesbah, Impact of heavy vehicles on surrounding traffic characteristics. *Journal of advanced transportation*, Vol. 49, No. 4, 2015, pp. 535–552.

[6] Alam, A., A. Gattami, and K. H. Johansson, An experimental study on the fuel reduction potential of heavy duty vehicle platooning. In *13th International IEEE Conference on Intelligent Transportation Systems*, IEEE, 2010, pp. 306–311.

[7] Aarts, L. and G. Feddes, European truck platooning challenge. In *HVTT14: International Symposium on Heavy Vehicle Transport Technology, Rotorua, New Zealand*, 2016.

[8] Bhoopalam, A. K., N. Agatz, and R. Zuidwijk, Planning of truck platoons: A literature review and directions for future research. *Transportation Research Part B: Methodological*, Vol. 107, 2018, pp. 212–228.

[9] Rijkswaterstaat, *European Truck Platooning Challenge 2016: Lessons Learnt*, 2016.

[10] Duret, A., M. Wang, and A. Ladino, A hierarchical approach for splitting truck platoons near network discontinuities. *Transportation Research Part B: Methodological*, 2019.

[11] Stefansson, E., J. F. Fisac, D. Sadigh, S. S. Sastry, and K. H. Johansson, Human-robot interaction for truck platooning using hierarchical dynamic games. In *European Control Conference (ECC)*, Naples, Italy, 2019.

[12] Jin, L., M. Čičič, S. Amin, and K. H. Johansson, Modeling the Impact of Vehicle Platooning on Highway Congestion: A Fluid Queuing Approach. In *Proceedings of the 21st International Conference on Hybrid Systems: Computation and Control (part of CPS Week)*, ACM, 2018, pp. 237–246.

[13] Wang, Y., E. B. Kosmatopoulos, M. Papageorgiou, and I. Papamichail, Local ramp metering in the presence of a distant downstream bottleneck: Theoretical analysis and simulation study. *IEEE Transactions on Intelligent Transportation Systems*, Vol. 15, No. 5, 2014, pp. 2024–2039.

[14] Hadiuzzaman, M., T. Z. Qiu, and X.-Y. Lu, Variable speed limit control design for relieving congestion caused by active bottlenecks. *Journal of Transportation Engineering*, Vol. 139, No. 4, 2012, pp. 358–370.

[15] Herrera, J. C., D. B. Work, R. Herring, X. J. Ban, Q. Jacobson, and A. M. Bayen, Evaluation of traffic data obtained via GPS-enabled mobile phones: The Mobile Century field experiment. *Transportation Research Part C: Emerging Technologies*, Vol. 18, No. 4, 2010, pp. 568–583.

[16] Cui, S., B. Seibold, R. Stern, and D. B. Work, Stabilizing traffic flow via a single autonomous

vehicle: Possibilities and limitations. In *Intelligent Vehicles Symposium (IV)*, IEEE, 2017, pp. 1336–1341.

[17] Wu, C., A. M. Bayen, and A. Mehta, Stabilizing traffic with autonomous vehicles. In *2018 IEEE International Conference on Robotics and Automation (ICRA)*, IEEE, 2018, pp. 1–7.

[18] Piacentini, G., P. Goatin, and A. Ferrara, Traffic control via moving bottleneck of coordinated vehicles. In *15th IFAC symposium on control in transportation systems*, 2018.

[19] Vinitsky, E., K. Parvatey, A. Kreidiehz, C. Wu, and A. Bayen, Lagrangian Control through Deep-RL: Applications to Bottleneck Decongestion. In *21st IEEE International Conference on Intelligent Transportation Systems (ITSC)*, Maui, US, 2018.

[20] Čičić, M. and K. H. Johansson, Traffic regulation via individually controlled automated vehicles: a cell transmission model approach. In *21st IEEE International Conference on Intelligent Transportation Systems*, Maui, US, 2018.

[21] Alam, A., B. Besselink, V. Turri, J. Martensson, and K. H. Johansson, Heavy-duty vehicle platooning for sustainable freight transportation: A cooperative method to enhance safety and efficiency. *IEEE Control Systems Magazine*, Vol. 35, No. 6, 2015, pp. 34–56.

[22] Liu, L., L. Zhu, and D. Yang, Modeling and simulation of the car-truck heterogeneous traffic flow based on a nonlinear car-following model. *Applied Mathematics and Computation*, Vol. 273, 2016, pp. 706–717.

[23] Delle Monache, M. L. and P. Goatin, Scalar conservation laws with moving constraints arising in traffic flow modeling: an existence result. *Journal of Differential equations*, Vol. 257, No. 11, 2014, pp. 4015–4029.

[24] Čičić, M. and K. H. Johansson, Stop-and-go Wave Dissipation Using Accumulated Controlled Moving Bottlenecks in Multi-class CTM Framework. In *Control and Decision Conference (ECC)*, Nice, France, 2019.

[25] Daganzo, C. F., The cell transmission model: A dynamic representation of highway traffic consistent with the hydrodynamic theory. *Transportation Research Part B: Methodological*, Vol. 28, No. 4, 1994, pp. 269–287.

[26] Piacentini, G., M. Čičić, A. Ferrara, and K. H. Johansson, VACS equipped vehicles for congestion dissipation in multi-class CTM framework. In *European Control Conference*, 2019.

[27] Kontorinaki, M., A. Spiliopoulou, C. Roncoli, and M. Papageorgiou, First-order traffic flow models incorporating capacity drop: Overview and real-data validation. *Transportation Research Part B: Methodological*, Vol. 106, 2017, pp. 52–75.

[28] Han, Y., Y. Yuan, A. Hegyi, and S. P. Hoogendoorn, New extended discrete first-order model to reproduce propagation of jam waves. *Transportation Research Record: Journal of the Transportation Research Board*, Vol. 2560, No. 1, 2016, pp. 108–118.